JOURNAL OF PROPULSION AND POWER
Vol. 10, No. 1, Jan.–Feb. 1994

Experimental Studies on Mixing of Two Co-Axial High-Speed Streams

A. K. Narayanan* and K. A. Damodaran†
Indian Institute of Technology, Madras 600 036, India

Currently, the focus of attention in aerospace propulsion research has been on the development of advanced air-breathing propulsion systems like scramjets, air-augmented rockets, multimode engines for the hyperplane, etc. A crucial technical problem to be tackled in such systems is the enhancement of mixing between two high-speed gaseous streams. Various methods have been tried so far, but the field is still very much an open one. Tests conducted earlier on subsonic flow mixing have shown that large-scale secondary flows, and not viscous diffusion, are the key to quick, low-loss, efficient mixing. In this regard, a lobe-type, convergent-divergent, supersonic nozzle, named the "Petal" nozzle, was designed, fabricated, and tested. Near-complete mixing with low total momentum loss within a short mixing chamber of length to diameter ratio of 4.35 was achieved.

Nomenclature

ata = atmospheres (absolute)
D = diameter
M = Mach number
m = axial momentum per unit area (momentum flux)
P = pressure
X = axial distance downstream from nozzle exit
ϕ = mixing factor

Subscripts
i = inner (primary) stream
major = major plane
minor = minor plane
o = outer (secondary) stream
s = static
t = throat of primary stream
ws = wall static

I. Introduction

RECENTLY, one can notice that considerable interest exists towards achieving enhanced mixing of two high-speed, gaseous streams. This has come about mainly in connection with the development of advanced propulsion systems such as scramjets, air-augmented rockets, etc.[1,2] Extremely short combustor residence time is a characteristic feature of these propulsion systems. The situation is further complicated by the fact that high Mach number, fully developed turbulent shear layers are associated with typically low shear-induced mixing.[3] Available data indicate a reduction in mixing rate by a factor of 3 between Mach numbers 1–5 due to compressibility effects.[4] Another point to consider is that shear-layer transition Reynolds number is high at high Mach numbers.[4] Therefore, in all advanced propulsion systems some techniques might have to be necessarily employed to enhance mixing between the primary stream, which may be pure fuel, premixed fuel/air, or hot fuel rich primary rocket exhaust and the secondary (air). They include 1) provision of increased mixing area, 2) control of shear-layer vorticity production, 3) imposition of swirl, 4) shock interaction, and 5) increased turbulence production, etc.[5] Significant improvement in mixing was observed by employing hypermixing nozzles[6] consisting of alternating flaps for the primary stream. But these were found to give rise to large mixing losses.

Considerable data, both experimental and theoretical, exist on the mixing of two high-speed streams using conventional, circular cross section or two-dimensional nozzles for the primary stream. In these cases potential core length estimates of the primary stream are seen to vary from 7 to 22 times the primary nozzle diameter depending on various test conditions.[7] Clearly, to achieve complete mixing and combustion using conventional nozzles, combustor lengths would have to be even longer. Recent work by Zhongqin et al.[8] has conclusively proved that primary nozzle geometry has a drastic influence on the mixing between the primary and secondary streams and subsequent combustion. Various geometries like rectangles,[9] ellipses,[10] etc., have been tried for the primary nozzle. In these cases some enhancement of mixing was found to occur, mainly due to azimuthal flow instabilities coupled with flow induction processes associated with elliptic vortices.

Tests conducted earlier for subsonic flows using lobe-type mixers have shown that large-scale secondary flows, not viscous diffusion, are the key to low-loss and efficient mixing.[11,12] In supersonic shear mixing layers, even though some large-scale, repetitive structures were observed, they do not appear to dominate the mixing layer character.[13] Using the mixer lobes, it is believed that very large-scale streamwise vortices are generated in the mixing duct, which causes the primary and secondary flows to mix rapidly and with low loss.[14] Lobe-type mixers have been employed successfully for subsonic applications like fan engines, ejectors, etc., to mix two streams in a short distance with little loss. In this regard, a high-penetration, lobe-type, convergent-divergent, supersonic nozzle was designed, fabricated, and tested. This nozzle, because of its flowerlike frontal view, was referred to as the Petal[15] nozzle. Air was used as working fluid for both streams. Two sets of tests were conducted: 1) mixing taking place in the open atmosphere[16] and 2) mixing occurring in cylindrical mixing chambers of various lengths. Results of these tests are presented in this article.

II. Description of Test Facility

The facility used for these tests can be divided into the following major subsystems: 1) air supply system, 2) test setup including the nozzles, and 3) instrumentation.

A. Air Supply System

It consists of the following components: 1) a two-stage, two-cylinder, water-cooled air compressor with intercooler and aftercooler and run by a 90-kW motor. It has a free air delivery

Received Sept. 26, 1992; revision received May 28, 1993; accepted for publication June 30, 1993.

*Research Scholar.
†Professor, Department of Aerospace Engineering.

rate of 8.5 m³/min with a maximum pressure of 18.5 ata; 2) three reservoirs with internal volume of 12-m³ each of design pressure 21 ata; and 3) a 152.4-mm-diam pipeline from the reservoir system to the test setup.

B. Test Setup

In the actual test setup, the main pipe supplies air to two lines, the primary (203.2-mm diam) and the secondary (101.6-mm diam) as shown in Fig. 1. The primary line ends in a contraction piece to which the nozzle to be tested can be screwed on. Air to the secondary nozzle is supplied through a settling chamber by means of four flexible rubber hoses. The primary and annular secondary flows mix within the mixing chamber located downstream of the two nozzles. For the first series of tests the mixing chamber was absent.

The petal-type convergent-divergent nozzle tested is designed for a critical pressure ratio of 5:1. A circular cross-sectional shape is maintained up to the throat. The nozzle has six troughs and six crests at the exit. In the plane of the trough (minor plane) the radial distance reduces from 11 mm at the throat to 5 mm at the exit, while in the plane of the crest (major plane) it increases from 11 to 20 mm. This has been done in order to obtain longer petal lobes for the specified area/pressure ratio. Provision has been made to screw the nozzle onto the setup. The outer flow takes place through the trough regions between the petal lobes and the shroud, with minimum area (throat) occurring in the same plane as the exit of the inner nozzle. The conical outer nozzle has an inlet diameter of 85 mm and exit diameter of 42 mm. A circular ring with internal threads was welded to the outer cone for attaching the mixing chamber. Mixing chambers of various lengths were made from acrylic tubes and threaded on one end to facilitate attachment to the ring.

C. Instrumentation and Testing

Blowing pressures of the primary and secondary streams were measured by pressure gauges (Fig. 1). A three dimensional traversing mechanism was employed to move the total/static probes axially and radially. Only mean flow quantities were measured. The probes were connected by plastic tubes to a diaphragm-type pressure transducer whose analog output was delivered to a calibrated digital interface unit. From total and static pressure measurements, after suitable shock correction, local mean flow properties like Mach number, axial momentum, etc., were calculated. For the open-mixing case, flow profiles at axial distances of X/D_t = 0, 0.91, 1.82, 2.73, and 3.64 in the major and minor planes were experimentally determined. For confined-mixing, flow profiles at the exit of cylindrical mixing tubes of length X/D_t = 1.82, 3.64, 5.46, 7.28, and 9.1 (corresponding to length/diameter ratios of mixing tubes of 0.87, 1.74, 2.60, 3.48, and 4.35, respectively) were determined.

III. Results and Discussion

To simulate an air augmented rocket under various operating conditions, total pressure of the outer flow was varied during the tests. The inner stream was maintained supersonic ($M \sim 1.65$) in all these tests by operating the petal nozzle at or above its critical pressure ratio.

A. Shadowgraphs

Figures 2a and 2b show shadowgraphs of the flow in the region of the petal nozzle exit in the major and minor planes, respectively, whereas Fig. 2c shows the corresponding shadow picture for a conventional, conical nozzle with same area ratio under similar test conditions. There is no secondary flow. These figures clearly bring out two striking features of the flow through a petal nozzle as compared to that of a conventional one, namely 1) the large divergence angle of the exit flow and 2) the near-linear increase of jet width in the major plane after the exit. The latter observation is particularly interesting since it is well known that the flow angle after the exit in a conventional, conical, convergent-divergent nozzle is dependent primarily on the static pressure and not the nozzle wall angle.[17] Another distinct feature is the central oblique shock (Fig. 2a) due to converging flow in the minor plane. In the central region, flow features of four petal lobes are superimposed on one another. This region is therefore seen as a complex pattern of Mach, shock, and expansion waves. Mach waves in the two vertical lobes can be seen in the outer regions in Fig. 2a.

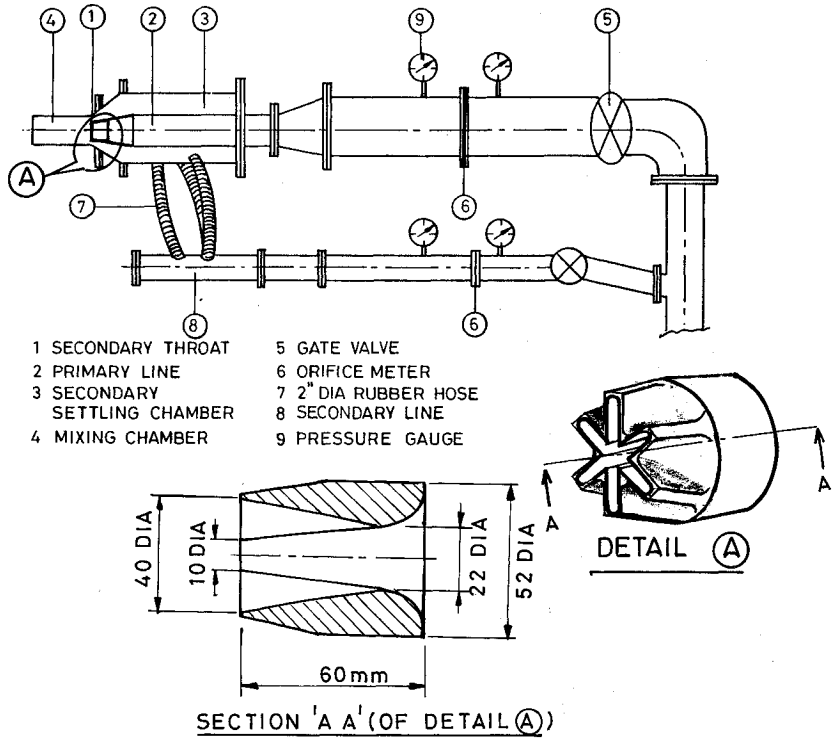

Fig. 1 Test setup.

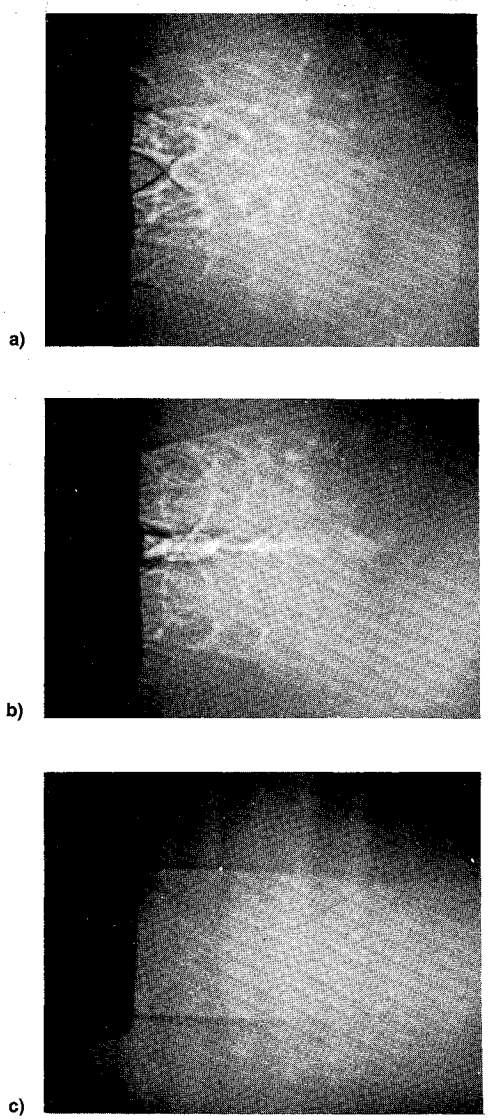

Fig. 2 Shadowgraphs (inner blowing pressure = 5 ata): a) petal nozzle (major plane), b) petal nozzle (minor plane), and c) conical nozzle.

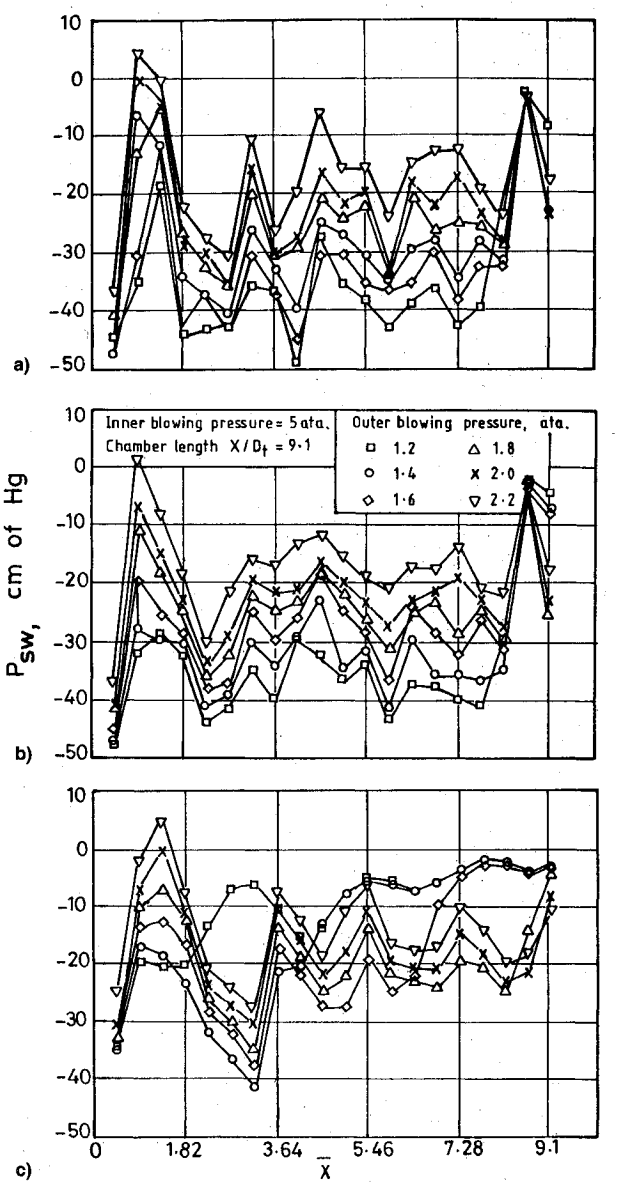

Fig. 3 Axial variation of wall static pressure: a) petal nozzle (major plane), b) petal nozzle (minor plane), and c) conical nozzle.

B. Wall-Static Pressure (Confined Mixing)

In confined flow studies, wall-static pressure variation along the mixing tube axis can provide useful information. Figures 3a and 3b show the axial variation of wall-static pressure in the major and minor planes, respectively, for P_i = 5 ata for various secondary blowing pressures. Figure 3c shows the corresponding variation for the conventional nozzle. Mixing chamber length is 20 cm (X/D_t = 9.1). These figures show that an increase in secondary pressure causes a general increase in static pressure at all axial locations. In the near zone, the presence of the outer flow brings about a compression of the inner flow as shown by the initial rise of P_{ws}. Thereafter, alternately decreasing and increasing wall-static pressure indicates the presence of typical supersonic-cell pattern in the flow. It may be noted that the first cell length is the same in all three figures. The second cell, however, is longer for the conventional nozzle. For higher outer pressures, a third and fourth cell are clearly seen for the conventional nozzle, while for the petal nozzle these are not distinct. Comparing the first cell in Figs. 3a and 3b, it is noted that the peak flow expansion point (corresponding to lowest static pressure) in the major and minor planes occur at X = 6 cm and X = 5 cm, respectively. This tangential variation of wall-static pressure could imply a crossflow between the two planes at that axial location.

C. Momentum Flux Profiles

Figure 4a shows radial distribution of axial momentum flux for the open-mixing case at five axial locations in the major plane, for various outer flow blowing pressures. Inner blowing pressure is 6 ata. At X/D_t = 1.82, momentum flux profiles in the major plane show the characteristic high-low-high (HLH) profile typical of the petal nozzle.[15] The profiles at X/D_t = 2.73 and 3.64 show that the outer parts of all the curves coalesce, signifying that the secondary flow does not affect these regions. The inner parts of the curves are seen to be strongly influenced by outer stream pressure. Higher pressures of the secondary flow is seen to result in greater primary flow momentum flux. The bulk of this momentum transfer, from minor to major plane, takes place in the region of the "low" point of the HLH profile. It may also be noted that the jet width in the major plane increases more or less linearly with axial distance as observed earlier from the shadowgraphs.

Figure 4b shows the corresponding radial distributions of momentum flux in the minor plane. It can be observed that the jet width in this plane decreases with axial distance indicating an outflux of momentum.

Figures 4c and 4d show the radial distribution of momentum flux for the confined-mixing case in the major and minor planes, respectively. These profiles are at once seen to be

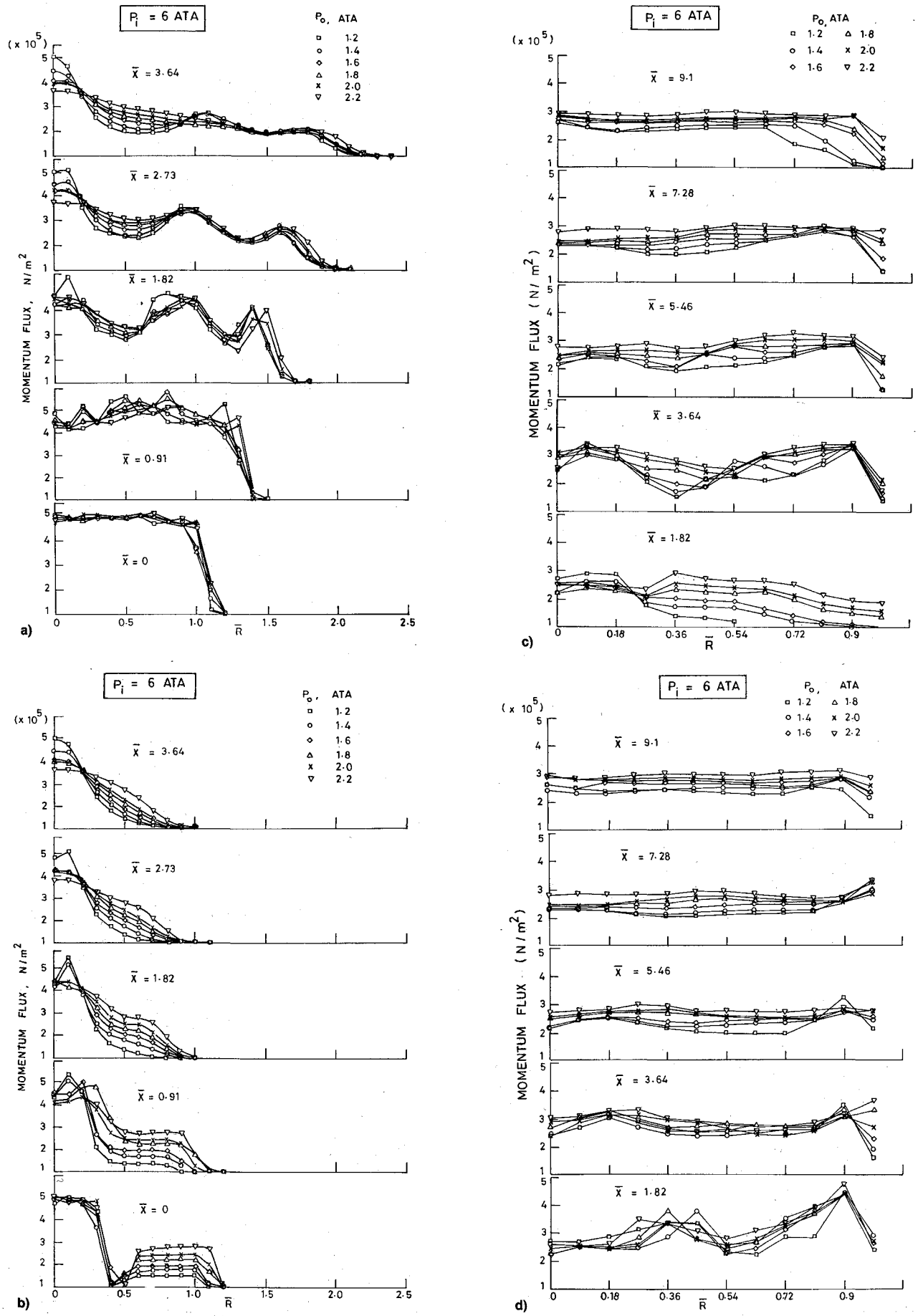

Fig. 4 Radial distribution of momentum flux along: a) major axis (open mixing), b) minor axis (open mixing), c) major axis (confined mixing), and d) minor axis (confined mixing).

significantly different from those for the open-mixing case. They show large momentum transfer from the major to the minor plane in contrast to the open-mixing case. Also, no distinct HLH profile is observable in the major plane. Momentum flux profiles in the major and minor planes at $X/D_t = 9.1$ for higher outer pressures show almost complete mixing.

Momentum flux profiles at $X/D_t = 1.82$ and 3.64 provide an insight into the rapid transfer of momentum from the major to minor plane. At $X/D_t = 1.82$, the major plane momentum flux profiles show a peak near the mixing tube wall, perhaps due to the presence of the mixing tube wall confining the jet spread in the major plane. As may be expected, this peak is seen to be independent of the secondary blowing pressure.

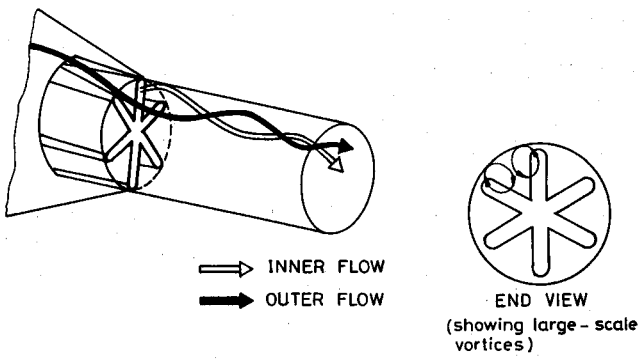

Fig. 5 Mixing mechanism.

The corresponding profiles at $X/D_t = 1.82$ for the minor plane show steady increase of momentum flux in the trough region with increasing secondary blowing pressure. There seems to be practically no momentum transfer from the primary thus far. But momentum flux profiles at $X/D_t = 3.64$ show an abrupt change. While the outer peak of momentum flux profile in the major plane has decreased considerably, the minor plane is seen to have gained momentum in the outer regions. Hence, these profiles show that a large transfer of momentum has taken place from the major to minor plane in the outer regions (i.e., near the mixing chamber wall). This is most likely due to large-scale vortices generated by the interaction of the divergent flow in the major plane and the mixing tube wall (Fig. 5). It is also conjectured that the breakup of the large-scale vortices to finer scales and subsequent shear mixing is responsible for the qualitative and quantitative similarity between the major and minor plane momentum flux profiles further downstream ($X/D_t = 9.1$). Another observation of interest is that higher secondary pressures seem to improve the mixing process. This is in contrast to what was observed in the conventional, conical nozzle, where higher secondary pressures are found to result in reduced mixing[18] for a given chamber length.

In order to supplement the above arguments and to have a better understanding of the initial stages in the mixing process, one can also examine the momentum flux profiles in the minor plane at $X/D_t = 3.64$ in Figs. 6a and 6b. It may be recalled that the large additional momentum flux in the minor plane is first observed at $X/D_t = 3.64$. Figure 6a shows the momentum flux profiles for open and confined mixing cases

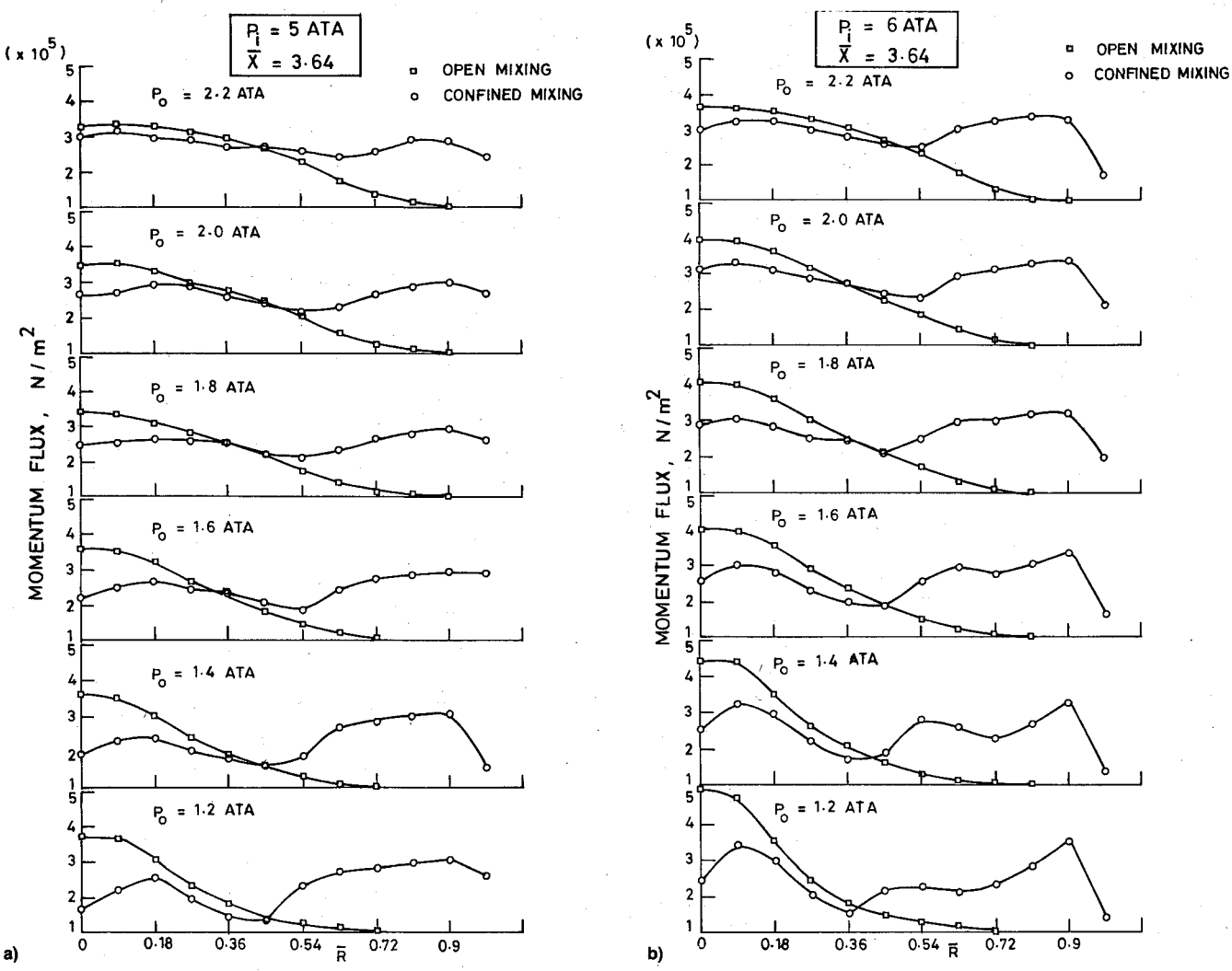

Fig. 6 Radial distribution of momentum flux along: a) minor axis ($X/D_t = 3.64$, $P_i = 5$ ata) and b) minor axis ($X/D_t = 3.64$, $P_i = 6$ ata).

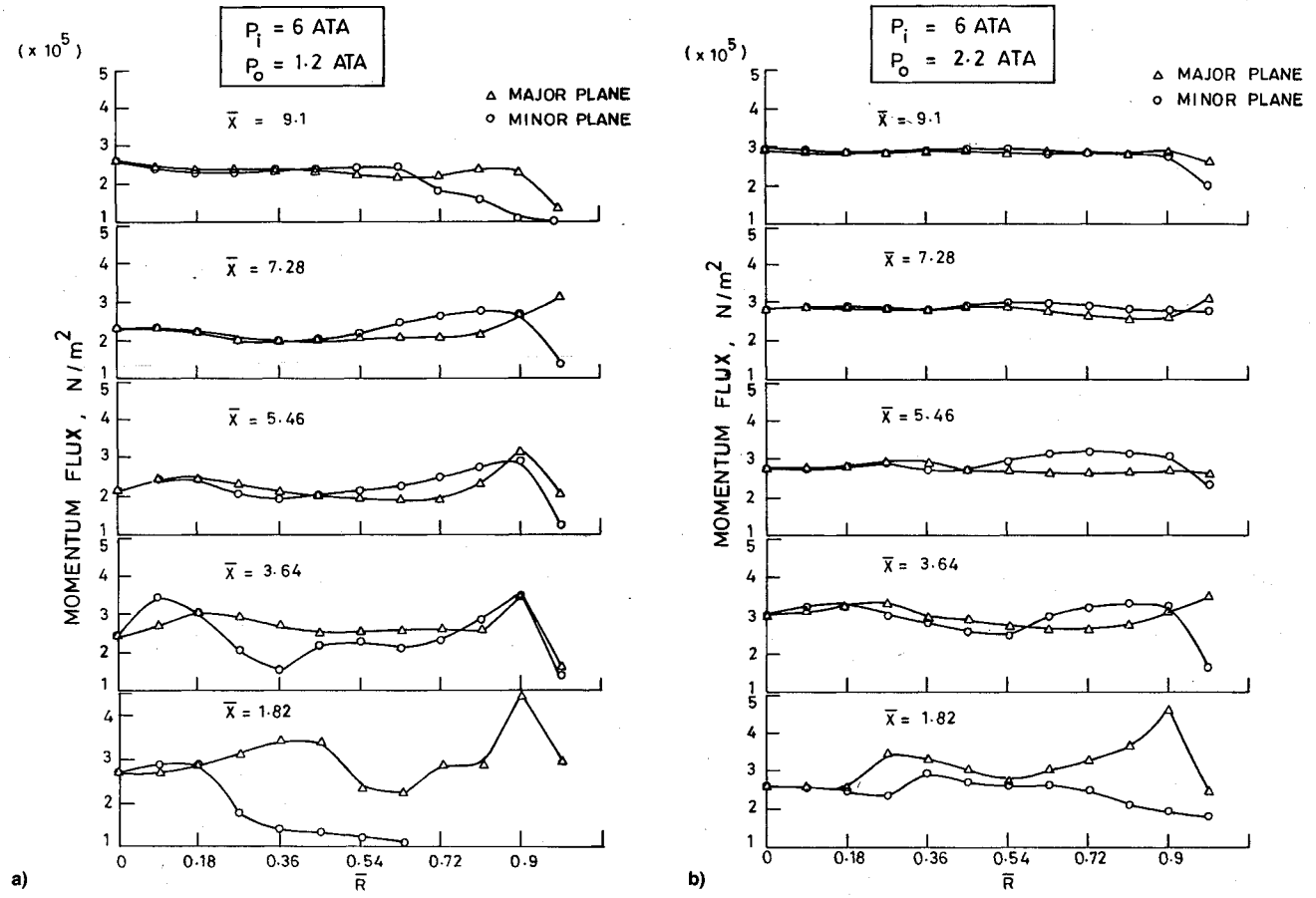

Fig. 7 Radial distribution of momentum flux: a) (confined mixing, P_o = 1.2 ata) and b) (confined mixing, P_o = 2.2 ata).

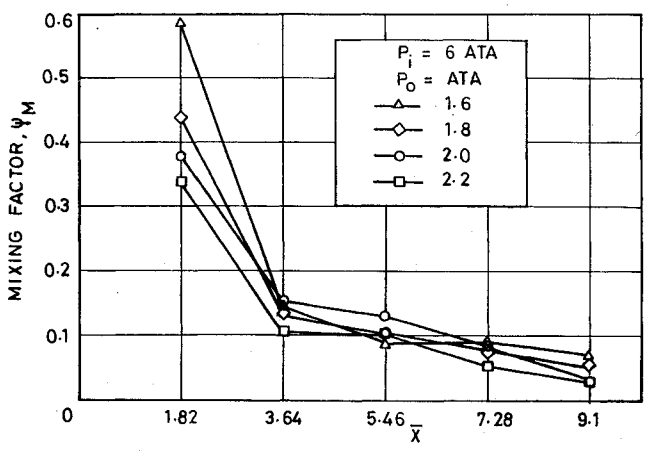

Fig. 8 Variation of mixing factor (P_i = 6 ata).

in the minor plane for primary blowing pressure of 5 ata. The extra momentum in the outer regions of the confined mixing curves is clearly seen. The peak value of this additional momentum is unaffected by changes in the secondary. Figure 6b shows the corresponding curves for primary blowing pressure of 6 ata. Again, it is observed that the outer peak is unaffected by changes in the secondary pressure. However, it may be noted that the outer peak value in Fig. 6a (primary blowing pressure = 5 ata) is less than that in Fig. 6b (primary blowing pressure = 6 ata). From the observation of all these momentum flux profiles it may be inferred that: 1) large additional momentum flux entering the outer regions of the minor plane at X/D_t = 3.64) is part of the primary flow; 2) this momentum flux was originally present in the outer regions of the major plane (X/D_t = 1.82); 3) this large-scale axial and tangential transfer of momentum could only have taken place due to large-scale vortices present near the wall of the mixing chamber; and 4) the fact that in the open-mixing case such a momentum transfer is absent shows the role of the mixing-tube wall in the generation of these large-scale vortices.

D. Mixing Profiles

The geometry of the petal nozzle makes it easy to quantify the mixing process in a simple manner. One has merely to observe the difference in momentum flux profiles in the major (primary flow) and minor (secondary flow) planes. Figures 7a and 7b show momentum profiles for the confined-mixing case at various axial locations in the major and minor planes. Primary blowing pressure is 6 ata and secondary pressures are 1.2 and 2.2 ata for Figs. 7a and 7b, respectively. It is observed that at X/D_t = 9.1, for secondary pressure of 2.2 ata, the two flows are almost fully mixed. Also, increasing outer pressure or having longer mixing chambers is seen to improve the mixing process. To quantify the mixing process, a mixing factor can be defined as

$$\phi = \left[\sum_{r=0}^{r=r_e} 4\left(\frac{m_{\text{major}} - m_{\text{minor}}}{m_{\text{major}} + m_{\text{minor}}}\right)^2\right]^{0.5}$$

e = edge of mixing chamber
$m = m(r)$

This implies that a decrease in the value of ϕ would denote better mixing, and for a completely mixed set of profiles, ϕ would be zero. Figure 8 shows the variation of ϕ with secondary blowing pressure and mixing chamber length. It may be noted that between chamber lengths of 40 mm (X/D_t = 1.82) and 80 mm (X/D_t = 3.64), there is a large drop in the value of ϕ. From X/D_t = 3.64 onwards, the decrease in ϕ is more gradual. This supplements earlier conclusions from the momentum flux profiles that large-scale momentum transfer takes place before X/D_t = 3.64. Downstream of this axial

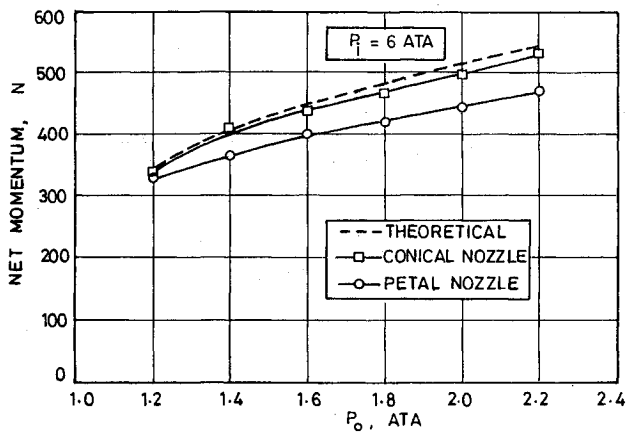

Fig. 9 Variation of net momentum (P_i = 6 ata).

location there is a decrease in the mixing rate as shown by the slope of ϕ vs mixing chamber length curves in Fig. 8. This can be attributed to the breakdown of large-scale vortices to smaller scales and subsequent shear mixing.

E. Net Momentum

In any mixing process an important criterion is the total pressure loss incurred. In propulsion systems for aerospace applications this assumes critical dimensions since the final thrust obtained is strongly dependent on the total pressure left for expansion after mixing and combustion.

From radial variation of momentum flux along the major and minor axes, net momentum of the flow exiting the mixing chambers was calculated by summing up the product of momentum flux and the area through which it is passing. Figure 9 shows variation of net-momentum with blowing pressure P_o for the petal and conventional conical nozzles under similar test conditions as compared with theoretically estimated values. It is observed that total momentum loss using a petal nozzle for the primary flow is around 10% at high outer flow blowing pressures, while there is practically no loss with the conventional, conical nozzle in comparison to the estimated values. This supplements earlier results[18] that very little mixing is taking place between the two streams in the case of the conventional nozzle, especially at higher outer flow pressures.

IV. Conclusions

Conclusions that may be drawn from these studies on mixing of two coaxial, high-speed streams using a petal nozzle for the primary flow are as follows:

A. Open-Mixing Case

Exit flow in the major plane of the petal nozzle has a large divergence angle which seems to be independent of primary blowing pressure. In the near region of the exit, this divergence angle is maintained and jet width in the major plane increases more or less linearly with axial distance. Changes in the outer flow blowing pressure seem to have little effect on flow in the central circular core in contrast to flow through the petal lobes. Momentum transfer takes place from the minor to major plane by shear mixing mainly in the region of the low point of the HLH profile.

B. Confined-Mixing Case

With an increase in outer flow blowing pressure there is a general increase in static pressure at all axial locations of the mixing chamber. It is believed that large-scale vortices are generated in the outer regions of the mixing chamber which rapidly transfer momentum from the major to the minor plane within a short distance of about four times the primary throat diameter. These vortices are generated by the interaction of the mixing chamber wall and the diverging flow in the major plane. The rate of momentum transfer decreases downstream, which can be attributed to the breakup of large-scale vortices to smaller ones and subsequent shear mixing. Increasing outer flow blowing pressure is found to improve the mixing process. Near-complete mixing within a short mixing chamber length of about nine times the throat diameter (or mixing tube L/D = 4.35) and with low total momentum loss (about 10%) can be achieved by using a petal nozzle for the primary flow.

Acknowledgments

The authors would like to express their sincere gratitude to M. R. Suresh, Research Associate and G. A. Venceslas, Technical Officer, Aerospace Engineering, Indian Institute of Technology, for invaluable help and useful discussions during all phases of this work. They are also thankful to C. M. Krishnakumar, undergraduate student, for help during the experimental phase of this work. This work was sponsored by the ISRO-IIT(M) cell.

References

[1]Thomas, A. N., "Return of the Ramjet," *Astronautics and Aeronautics*, Jan. 1984.

[2]Thomas, A. N., "New Generation Ramjets—A Promising Future," *Astronautics and Aeronautics*, June 1980.

[3]Chinzei, N., Masuya, G., Komuro, T., Murakami, A., and Kudou, K., "Spreading of Two-Stream Supersonic Turbulent Mixing Layers," *Physics of Fluids*, May 1986, pp. 1345–1347.

[4]Birch, S. F., and Keyes, J. W., "Transition in Compressible Free Shear Layers," *Journal of Spacecraft and Rockets*, Vol. 9, No. 8, 1972, pp. 623, 624.

[5]Kumar, A., Bushnell, D. M., and Hussaini, M. Y., "Mixing Augmentation Technique for Hypervelocity Scramjets," *Journal of Propulsion and Power*, Vol. 5, No. 5, 1989, pp. 514–522.

[6]Bevilaqua, P. M., "Evaluation of Hypermixing for Thrust Augmenting Ejectors," *Journal of Aircraft*, Vol. 11, June 1974, pp. 348–354.

[7]Forde, J. M., "The Mixing of Turbulent Supersonic Fuel-Air Streams," *Aeronautical Quarterly*, Nov. 1965, pp. 377–387.

[8]Zhongqin, Z., Zhenpeng, Z., Jinfu, T., and Wenlan, F., "Experimental Investigation of Combustion Efficiency of Air-Augmented Rockets," *Journal of Propulsion and Power*, Vol. 2, No. 4, 1986, pp. 305–310.

[9]Hsia, Y. C., Krothapalli, A., and Baganoff, D., "Mixing of an Underexpanded Rectangular Jet Ejector," *Journal of Propulsion and Power*, Vol. 4, No. 3, 1988, pp. 256–262.

[10]Schadow, K. C., Gutmark, E., Wilson, K. J., and Parr, D. M., "Mixing Characteristics of a Ducted Elliptical Jet," *Journal of Propulsion and Power*, Vol. 4, No. 4, 1988, pp. 328–333.

[11]Werle, M. J., Vatsa, V. H., Kardas, G. F., and Presz, W. M., "Turbofan Forced Mixer-Nozzle Internal Flowfield," Final Rept., NASA Contract NAS3-2091, Vol. 2, April 1981.

[12]Paterson, R. W., "Turbofan Mixer Nozzle Internal Flowfield—A Benchmark Experimental Study," Transactions of American Society of Mechanical Engineers, *Journal of Engineering for Gas Turbines and Power*, Vol. 106, July 1984.

[13]Goebel, G., Dutton, J. C., Krier, H., and Renie, J. P., "Mean and Turbulent Velocity Measurements of Supersonic Mixing Layers," *Experiments in Fluids*, Vol. 8, No. 3, 1990, pp. 263–272.

[14]Presz, W. M., Morin, B. L., and Gousy, R. G., "Forced Mixer Lobes in Ejector Designs," *Journal of Propulsion and Power*, Vol. 4, No. 4, 1988, pp. 350–355.

[15]Narayanan, A. K., and Damodaran K. A., "Experimental Investigations on Flow Through a Petal Nozzle," *Journal of the Institution of Engineers*, No. 3, 1990, pp. 1–4.

[16]Narayanan, A. K., and Damodaran, K. A., "Mixing Characteristics of Flow Through a Petal Nozzle with a Secondary Stream," *Proceedings of the 17th National Conference (India) on Fluid Mechanics and Fluid Power*, No. 12, 1990.

[17]Adamson, T. C., and Nicholls, J. A., "On the Structure of Jets from Highly Underexpanded Nozzles Into Still Air," *Journal of Aerospace Sciences*, 1959, pp. 16–24.

[18]Narayanan, A. K., and Damodaran, K. A., "Confined Mixing of Two Isothermal Axisymmetric Airstreams," *Proceedings of the Seventeenth National Conference (India) on Fluid Mechanics and Fluid Power*, No. 12, 1990.